# Spin−Orbit and Relativistic Effects on Structures and Stabilities of Group 17 Fluorides $EF_3$ (E = I, At, and Element 117): Relativity Induced Stability for the $D_{3h}$ Structure of $(117)F_3$

**Cheolbeom Bae,[†] Young-Kyu Han,[‡] and Yoon Sup Lee*[,†]**

*Department of Chemistry and School of Molecular Science (BK21), Korea Advanced Institute of Science and Technology, Daejon 305-701, Korea, and Analytical and Computational Science, LG Chem, Ltd., Research Park, Daejeon 305-380, Korea*

*Received: July 15, 2002; In Final Form: October 24, 2002*

Spin−orbit and scalar relativistic effects on geometries, vibrational frequencies, and energies for group 17 fluorides $EF_3$ (E = I, At, and element 117) are evaluated with two-component methods using relativistic pseudopotentials and effective one-electron spin−orbit operators. The inclusion of relativistic effects makes the $D_{3h}$ structure of $(117)F_3$ a stable local minimum, whereas $IF_3$ and $AtF_3$ retain $C_{2v}$ local minima even with relativistic effects. The valence shell electron pair repulsion model is not appropriate to explain the molecular structure of $(117)F_3$. The geometries of $EF_3$ (E = I, At, and element 117) molecules are optimized at the HF level with and without spin−orbit effects. Spin−orbit interactions elongate the bond lengths and decrease the harmonic vibrational frequencies. In the case of $AtF_3$, spin−orbit interactions increase the bond lengths by 0.044 and 0.023 Å for $r_e^{eq}$ and $r_e^{ax}$, respectively. Spin−orbit effects widen the bond angle of $C_{2v}$ structures of $IF_3$ and $AtF_3$, i.e., spin−orbit effects diminish the second-order Jahn−Teller term. The bond angle $\alpha_e$ of $AtF_3$ increases by 3.9° due to spin−orbit interactions in addition to the increase of 4.8° by scalar relativistic effects. For $(117)F_3$, spin−orbit effects increase the bond length by 0.109 Å. The spin−orbit interactions stabilize $(117)F_3$ by a significant margin (∼1.2 eV). This stabilization of the molecule compared with open p-shell atoms is quite unusual. Enhanced ionic bonding may be responsible for this stabilization because the electronegative F atom can effectively polarize or attract electrons from the destabilized $7p_{3/2}$ spinors of element 117 due to huge spin−orbit splitting of 7p.

## 1. Introduction

Group 17 element fluorides $EF_3$ are well-known to have a bent T $C_{2v}$ structure instead of a trigonal planar $D_{3h}$ structure, which can be explained by the valence shell electron pair repulsion theory (VSEPR)[1−3] or the second-order (or pseudo-) Jahn−Teller (SOJT) concept.[4−15] Hoyer and Seppelt[16] obtained $IF_3$ in the form of very thin, yellow platelets, which construct a polymeric structure. The coordination polyhedron around the iodine atom is a planar pentagon with two weak intramolecular I−F···I bonds in addition to three covalent I−F bonds. A single-crystal X-ray structure determination of $IF_3$ shows that a planar T-shaped $C_{2v}$ molecule can be derived from the polymeric structure on considering only the shortest three I−F bonds.[16] There are only a few calculations on $IF_3$.[17−20] The intermolecular bonding in dimers of the T-shaped hypervalent $XF_3$ (X = Cl, Br, and I) compounds is analyzed using a combination of density functional calculations.[19] Schwerdtfeger[20] investigated scalar relativistic effects in the F−E−F distortion angles, bond distances, harmonic vibrational frequencies, and decomposition energies of $EF_3$ (E = Cl, Br, I, and At), reporting that scalar relativistic effects diminish the SOJT term and induce a substantial increase in the $F_{eq}$−E−$F_{ax}$ bond angles of 5.5° for $AtF_3$. Schwerdtfeger also suggested that a more sophisticated configuration interaction (CI) procedure including spin−orbit coupling would be necessary to obtain an accurate theoretical structure for $AtF_3$. Although a new transactinide element of group 17, element 117, is yet to be observed, relativistic effects on (117)H were calculated at the mass−velocity and Darwin (MVD) and four-component Dirac−Hartree−Fock (DHF) levels of theory by Saue et al.,[21] at the spin−orbit CI level by Nash and Bursten,[22] and at the two-component coupled cluster (CC) level of theory by Han et al.[23,24] Recently, Fægri and Saue explored the relativistic effects on the diatomic molecules containing element 117 such as Tl(117) and (113)(117) at the DHF level of theory.[25]

Accurate theoretical descriptions of the electronic structures of heavy atoms and molecules require consideration of spin−orbit interactions in addition to scalar relativistic effects. It was reported for the first time by Nash and Bursten[26] that spin−orbit effects on the bonding in $(118)F_4$ is large enough to induce the stability of a non-VSEPR $T_d$ structure, which was also the conclusion of Han et al.[27] Relativistic effective core potentials or pseudopotentials (PP) can conveniently handle relativistic effects such as scalar relativistic effects and spin−orbit effects for molecules containing such heavy atoms without the inclusion of core electrons.[28] There are many variants of methods to consider spin−orbit interactions in relativistic representation of electrons. An approach of using two-component spinors, in which PPs including spin−orbit interactions are treated from the Hartree−Fock (HF) step, may have advantages in some cases.[29−32] It is simple to obtain spin−orbit effects from two-component results in the geometries, energies, and properties at the HF level.

* Corresponding author. E-mail: yslee@mail.kaist.ac.kr. Phone: 82-42-869-2821. Fax: 82-42-869-2810.
† Korea Advanced Institute of Science and Technology.
‡ LG Chem, Ltd..

10.1021/jp026531m CCC: $25.00 
Published on Web 01/18/2003

Spin–orbit effects on group 17 element fluoride $EF_3$ compounds have not been investigated so far, although spin–orbit splittings are largest for the group 17 elements (~0.9 eV for I, ~2.9 eV for At, and ~8.6 eV for element 117).[33] We apply the two-component geometry optimization[34] to the $EF_3$ (E = I, At, and element 117) molecules. The optimized geometries are investigated by normal-mode analysis[27] to ensure that obtained geometries are minima. We study the spin–orbit effects on the structures and vibrational frequencies of $EF_3$ (E = I, At, and element 117) molecules. Spin–orbit and electron correlation energies are calculated at the Møller–Plesset second-order perturbation (MP2), coupled cluster singles and doubles (CCSD), and CCSD with perturbed triples [CCSD(T)] levels of theory. The atomization and decomposition reaction energies are investigated. Spin–orbit effects on the molecular structures, vibrational frequencies, stabilities, and SOJT term are discussed. We perform the nonrelativistic PP (NRPP) calculations in addition to the relativistic PP calculations, to estimate the scalar relativistic effects on the $EF_3$ (E = I, At, and element 117) molecules. The present result indicates that VSEPR is not valid for the $(117)F_3$ molecule because $(117)F_3$ has a trigonal planar $D_{3h}$ structure in relativistic calculations.

## 2. Computational Details

We have developed the two-component Kramers' restricted HF (KRHF) method,[29] which includes spin–orbit interactions at the HF level of theory using PPs. The KRHF program utilizes the PPs with effective one-electron spin–orbit operators (SOPP) at the HF level and produces molecular spinors obeying double group symmetry. The KRHF method can be a starting point for many single reference correlated methods of treating spin–orbit interactions. We have implemented MP2, CI, and CC methods based upon the KRHF molecular spinors and designated them as KRMP2, KRCI, and KRCC methods, respectively.[29–32,35] When the spin–orbit effects are substantial as in the case of element 117, it may be possible to recover larger portions of the electron correlation energies from the post-HF calculations based on the reference state generated in the presence of spin–orbit interactions than from those neglecting spin–orbit interactions. We have implemented two-component geometry optimization and normal-mode analysis using analytic gradient.[27,34] With the KRHF geometry optimization program, we can optimize the structures of polyatomic molecules at the HF level explicitly treating spin–orbit interactions.

The 7 valence electron (VE) energy-adjusted pseudopotentials (EAPP) and corresponding 5s5p1d valence basis sets were used for iodine and astatine.[36] For element 117, the 25 VE EAPP and 8s8p6d4f basis set were used.[37] A reduced basis set of 8s8p6d1f (f = 1.236) was used in SOPP calculations of harmonic vibrational frequencies and atomization energies of $(117)F_3$ for practical reasons. For the F atom, 6-311+G* basis sets were used[38] and 1s core orbitals were excluded at all correlated levels of theory employed here. In SOPP calculations for atomization energies of $(117)F_3$, spinors with orbital energies higher than 50 au were omitted in the correlation calculation because virtual orbitals with high orbital energies have been found to contribute very little to correlation effects in the scalar-relativistic calculations of $(117)F_3$ with spin–orbit averaged scalar relativistic PP (ARPP).

Atomization energies were evaluated using results of separate calculations for atoms. All structures optimized using analytic gradients at the HF level were verified to be minima by computing the matrix of energy second derivatives and performing normal-mode analysis. For EF (E = I, At, and element 117), bond lengths and harmonic vibrational frequencies were obtained from Dunham analysis. The spinor Mulliken populations were calculated and the natural bond orbital (NBO) analysis methods[39] are utilized to analyze the bond nature of $(117)F_3$ in NRPP and ARPP calculations.

Spin–orbit effects are defined as the difference between the spin-averaged one-component ARPP and the two-component SOPP results calculated with the same basis set at a given level of theory. Scalar relativistic effects are defined as the difference between the ARPP and NRPP results. NRPP and ARPP calculations were carried out with the GAUSSIAN98[40] and MOLPRO98[41] whereas SOPP calculations were performed with two-component packages on CRAY C90 at KISTI.

**TABLE 1: HF and KRHF Optimized Geometries of $EF_3$ (E = I, At, and Element 117)[a]**

| | method | $C_{2v}$ $r_e^{eq}$ | $C_{2v}$ $r_e^{ax}$ | $C_{2v}$ $\alpha_e$ | $D_{3h}$[b] $r_e$ |
|---|---|---|---|---|---|
| $IF_3$ | ARPP-HF | 1.875 | 1.959 | 83.1 | (1.972) |
| | SOPP-KRHF | 1.879 | 1.961 | 83.2 | (1.976) |
| | exp[c] | 1.872 | 1.983 | 80.2 | |
| $AtF_3$ | ARPP-HF | 1.981 | 2.079 | 84.8 | (2.075) |
| | SOPP-KRHF | 2.025 | 2.102 | 88.7 | (2.103) |
| $(117)F_3$ | NRPP-HF | 2.015 | 2.076 | 77.7 | (2.084) |
| | ARPP-HF | | | | 2.109 |
| | SOPP-KRHF | | | | 2.218 |

[a] Bond distances are in angstroms, and angles are in degrees. [b] The $r_e$'s in parentheses are found to be first-order transition states. [c] The geometry from X-ray crystallography in ref 16.

## 3. Results and Discussion

The ARPP and SOPP optimized geometries of the group 17 fluorides $EF_3$ (E = I, At, element 117) at the HF level of theory are listed in Table 1. There are three probable geometries, bent T $C_{2v}$, pyramidal $C_{3v}$, and trigonal planar $D_{3h}$, from symmetry consideration. For five valence electron pairs on the central group 17 element, VSEPR predicts a $C_{2v}$ structure for this molecule. We examined $C_{2v}$, $D_{3h}$, and $C_{3v}$ structures but could not find any local minimum in $C_{3v}$ symmetry. The $C_{2v}$ and $D_{3h}$ structures and their bond axes, $r_e^{eq}$, $r_e^{ax}$, and $r_e$, and their bond angle $\alpha_e$ are defined in Figure 1. For $IF_3$ and $AtF_3$, $C_{2v}$ structures are found to be local minima, and $D_{3h}$ structures to be first-order transition states in scalar relativistic ARPP calculations, which is in agreement with the results of Schwerdtfeger.[20] Even with spin–orbit effects, we found that $C_{2v}$ structures of $IF_3$ and $AtF_3$ remain as local minima and $D_{3h}$ structures of them remain as first-order transition states. In the case of $(117)F_3$, although the $C_{2v}$ structure describes a local minimum in the nonrelativistic calculation, adding the scalar-relativistic effects or both the scalar relativistic and spin–orbit effects results in a $D_{3h}$ structure as local minimum. This is the first molecule of the group 17 element for which the shape of most stable isomer changes by the scalar relativistic effects, although spin–orbit induced stability for the $T_d$ structure of $(118)F_4$ has been reported.[26,27] Normal-mode analyses were performed at the HF optimized geometries using ARPPs and SOPPs. Table 2 and Table 3 list the HF harmonic vibrational frequencies of $EF_3$ (E = I, At, element 117) for $C_{2v}$ and $D_{3h}$, respectively. The vibrational frequencies in Tables 2 and 3 reveal that the optimized geometries are local minima or first-order saddle points.

The SOPP bond lengths of $IF_3$ are 1.879 and 1.961 Å for $r_e^{eq}$ and $r_e^{ax}$, respectively, and the SOPP bond angle $\alpha_e$ is 83.2° at the HF level. The $C_{2v}$ structure of $IF_3$ has 1.872 Å for $r_e^{eq}$, 1.983 Å for $r_e^{ax}$, and 80.2° for $\alpha_e$ from a single-crystal X-ray

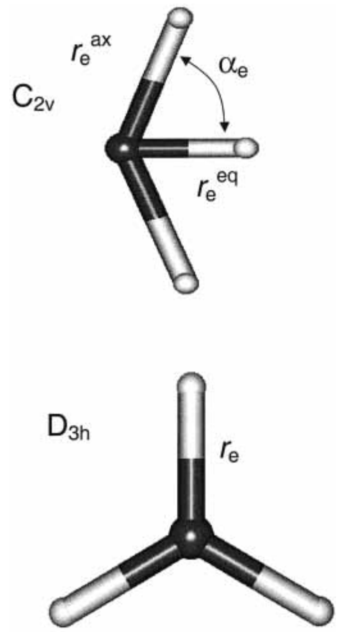


**Figure 1.** Bent T $C_{2v}$ and planar $D_{3h}$ geometries of $EF_3$ (E = I, At, and element 117).

structure.[16] The calculated structure is similar to the single-crystal X-ray structure. The SOPP bond lengths of $AtF_3$ are 2.025 and 2.076 Å for $r_e^{eq}$ and $r_e^{ax}$, respectively, which are longer than those of $IF_3$ by about 0.14 Å. The SOPP bond angle $\alpha_e$ of $AtF_3$ is 88.7°. It is noteworthy that the bond angle $\alpha_e$ increases by 3.9° with the inclusion of spin−orbit effects at the HF level.

All stretching modes have vibrational frequencies larger than those of out-of-plane and bending modes by about 400 cm$^{-1}$. Spin−orbit effects decrease the harmonic vibrational frequencies in all the cases, as shown in Tables 2 and 3. The spin−orbit induced reduction of harmonic vibrational frequencies increases from iodine to element 117, as expected. The changes of frequencies due to spin−orbit interactions for $IF_3$ are negligible. For the bending modes of $AtF_3$, spin−orbit changes of the harmonic vibrational frequencies are 30% and 25% for $\nu_2(A_1)$ symmetric and $\nu_3(B_2)$ asymmetric bending mode, respectively. In the case of $(117)F_3$, spin−orbit changes of $\nu_1(E')$ bending and $\nu_2(A_2'')$ out-of-plane bending modes are 45% and 75%, respectively. The $\nu_1(E')$ bending mode shows that the $D_{3h}$ structures of $IF_3$ and $AtF_3$ are first-order transition states regardless of spin−orbit effects. Spin−orbit interactions decrease $\nu_2(A_2'')$ out-of-plane bending, $\nu_3(E_2')$ asymmetric stretching, and $\nu_4(A_1')$ symmetric stretching modes by about 30 cm$^{-1}$, but do not affect the $\nu_1(E')$ bending frequencies of $IF_3$ and $AtF_3$.

Spin−orbit and scalar relativistic effects on the structures of $EF_3$ (E = I, At, and element 117) are compiled in Table 4. Scalar relativistic effects on the structure of $IF_3$ and $AtF_3$ are from Schwerdtfeger's results.[20] Compared with scalar relativistic effects, spin−orbit effects on the structure of $IF_3$ are negligible. The geometric $\Delta_{SO}$ of $IF_3$ is less than 10% of those due to scalar relativistic effects. In the case of $AtF_3$, spin−orbit interactions increase the bond lengths by 0.044 and 0.023 Å for $r_e^{eq}$ and $r_e^{ax}$, respectively, whereas scalar relativistic effects increase $r_e^{eq}$ by 0.023 Å and $r_e^{ax}$ by 0.041 Å. The bond angle $\alpha_e$ increases by 3.9° due to spin−orbit interactions in addition to the increase of 4.8° due to scalar relativistic effects.

Due to $a_1'$ HOMO ⊗ e′ LUMO mixing at the highly symmetric trigonal planar $D_{3h}$ structure, the group 17 fluorides $EF_3$ (E = Cl, Br, I, and At) distort into bent T-shaped $C_{2v}$ arrangements, which is the mechanism of SOJT. The 3.9° increase of the bond angle $\alpha_e$ due to spin−orbit interactions could also be explained by the SOJT term. The leading part in the SOJT term[8−15,20] is

$$\langle\psi_0|\left(\frac{\partial^2 H}{\partial Q_i^{\,2}}\right)_0|\psi_0\rangle + 2\sum_k \frac{|\langle\psi_k|\left(\frac{\partial H}{\partial Q_i}\right)_0|\psi_0\rangle|^2}{V_0 - V_k}$$

which contributes to the energy relaxation of a molecular system by mixing the *k*th excited state into the ground state through geometrical distortion to the direction of $Q_i$. Here $\psi_0$ and $\psi_k$ are the electronic wave functions of the ground and *k*th excited state, respectively, and $V_0$ and $V_k$ are their corresponding adiabatic energies. The denominator, $(V_0 - V_k)$, is approximately estimated from HOMO−LUMO energy gaps. As the HOMO−LUMO energy gap in the denominator of the SOJT term becomes larger, the SOJT distortion is expected to decrease. The HOMO−LUMO gaps at the partially optimized geometries are plotted against bond angle α in Figure 2. When spin−orbit interactions are included using SOPP, the HOMO−LUMO gap for molecular spinors of $AtF_3$ widens by 0.017 au at the ARPP optimized geometry. The bond angle α of $AtF_3$ relaxes to 88.7° on the SOPP potential energy surface. As the larger HOMO−LUMO gaps for SOPP than for ARPP lead to the smaller SOJT distortion for the former, the bond angle $\alpha_e$ is larger for the former than the latter by 3.9°. It is noted that the contribution of the first term of SOJT is not considered here.

Spin−orbit interactions increase the bond length, $r_e$ of (117)-$F_3$ by 0.109 Å. The bond elongation for the $p_{3/2}$ valence molecules can be explained by the expansion of the $p_{3/2}$ spinor due to the spin−orbit splitting of 7p. The bond elongation phenomenon for the $p_{3/2}$ valence molecules also appears in the molecules containing sixth-row elements with open-shell p electrons such as Bi, Po, and At[34,42] and seventh-row transactinide element congeners.[24]

The ARPP and SOPP atomization energies (AE) calculated at the HF, MP2, CCSD, and CCSD(T) levels of theory are summarized in Table 5. All correlation calculations were performed at the HF optimized geometries. The SOPP atomization energies of $IF_3$, $AtF_3$, and $(117)F_3$ are 5.61, 5.67, and 8.49 eV at the CCSD(T) level of theory, respectively. The atomization energy of $(117)F_3$ is larger by quite a large margin, about 2.85 eV, than almost the same atomization energies of $IF_3$ and $AtF_3$. Whereas the atomization energy of $(117)F_3$ increases due to spin−orbit effects, the atomization energies of $IF_3$ and $AtF_3$ decrease. The $\Delta_{SO}$(AE)'s of $IF_3$ and $AtF_3$ are less than 5% of the atomization energies. In the case of $IF_3$, the spin−orbit effects on the atomization energies are −0.24 eV, insensitive to the electron correlation effects. Changes of the atomization energies due to electron correlations are 4.49 eV with or without spin−orbit effects, implying an additivity of spin−orbit and electron correlation effects. The magnitude of spin−orbit effects $\Delta_{SO}$(AE) is smaller for $AtF_3$ than for $IF_3$ whereas the additivity of spin−orbit and electron correlation effects becomes less apparent for $AtF_3$. The spin−orbit effect on the atomization energy of $(117)F_3$ is +1.24 at the CCSD(T) level, which is about 15% of the large atomization energy (8.49 eV). The change of atomization energy due to spin−orbit effects depends on where the stabilization induced by spin−orbit effects is more effective. In the case of $(117)F_3$, the stabilization by spin−orbit interaction is more dominant in the bonding molec-

**TABLE 2: Harmonic Vibrational Frequencies ($cm^{-1}$) of $EF_3$ (E = I, At, and Element 117) for the $C_{2v}$ Symmetry at the HF Level of Theory**

| | method | $\nu_1(B_1)$ out of plane | $\nu_2(A_1)$ sym bend | $\nu_3(B_2)$ asym bend | $\nu_4(A_1)$ sym str | $\nu_5(B_2)$ asym str | $\nu_6(A_1)$ sym str |
|---|---|---|---|---|---|---|---|
| $IF_3$ | ARPP-HF | 219 | 215 | 319 | 593 | 605 | 709 |
| | SOPP-KRHF | 217 | 212 | 315 | 589 | 603 | 702 |
| | $\Delta_{SO}$[a] | −2 | −3 | −4 | −4 | −2 | −7 |
| $AtF_3$ | ARPP-HF | 188 | 144 | 254 | 566 | 537 | 650 |
| | SOPP-KRHF | 164 | 109 | 202 | 541 | 521 | 587 |
| | $\Delta_{SO}$[a] | −24 | −35 | −52 | −25 | −16 | −63 |
| $(117)F_3$ | NRPP-HF[b] | 158 | 192 | 287 | 580 | 582 | 658 |

[a] The $\Delta_{SO}$ values are defined by the SOPP frequency minus ARPP frequency. [b] The frequencies are calculated using the 4f basis on element 117.

**TABLE 3: Harmonic Vibrational Frequencies ($cm^{-1}$) of $EF_3$ (E = I, At, and Element 117) for the $D_{3h}$ Symmetry at the HF Level of Theory[a]**

| | method | $\nu_1(E')$ bend | $\nu_2(A_2'')$ out of plane | $\nu_3(E_2')$ asym str | $\nu_4(A_1')$ sym str |
|---|---|---|---|---|---|
| $IF_3$ | ARPP-HF | −122 | 295 | 567 | 601 |
| | SOPP-KRHF | −122 | 289 | 563 | 596 |
| $AtF_3$ | ARPP-HF | −31 | 237 | 542 | 581 |
| | SOPP-KRHF | −31 | 197 | 518 | 546 |
| $(117)F_3$ | NRPP-HF[b] | −54 | 241 | 565 | 578 |
| | ARPP-HF | 84 | 193 | 544 | 580 |
| | SOPP-KRHF | 58 | 110 | 475 | 497 |
| | $\Delta_{SO}$[a] | −26 | −83 | −69 | −83 |

[a] The $\Delta_{SO}$ values are defined by the SOPP frequency minus ARPP frequency. [b] The frequencies are calculated using the 4f basis on element 117.

**TABLE 4: Relativistic Effects (Spin−Orbit Effects and Scalar Relativistic Effects) on Geometries of $EF_3$ (E = I, At, and Element 117) at the HF Level of Theory[a]**

| | spin−orbit effects | | | | scalar relativistic effects | | |
|---|---|---|---|---|---|---|---|
| | $C_{2v}$ | | | $D_{3h}$ | $C_{2v}$ | | |
| | $r_e^{eq}$ | $r_e^{ax}$ | $\alpha_e$ | $r_e$ | $r_e^{eq}$ | $r_e^{ax}$ | $\alpha_e$ |
| $IF_3$ | 0.004 | 0.002 | 0.1 | | −0.052 | 0.107 | 0.9 |
| $AtF_3$ | 0.044 | 0.023 | 3.9 | | 0.023 | 0.041 | 4.8 |
| $(117)F_3$ | | | | 0.109 | | | |

[a] Bond distances are in angstroms, and angles are in degrees. Spin−orbit effects are defined by the SOPP value minus the ARPP value, and scalar relativistic effects are defined by the ARPP value minus the NRPP value. Scalar relativistic effects are from ref 20.

ular region than in the dissociated atomic regions. The enormous stabilization caused by spin−orbit effects can be explained mainly by the radial expansion and energetic destabilization of the $7p_{3/2}$(SOPP) spinors compared with the 7p(ARPP) orbitals. The expanded $7p_{3/2}$ may allow better overlap with atomic orbitals or spinors of the F atom resulting in a stronger bond. The electronegative F atom can effectively polarize or attract electrons from the energetically destabilized $7p_{3/2}$ spinors of $(117)F_3$, as can be seen in the Mulliken population analysis in Table 6. The spin−orbit effects reduce the total electron population of 7p spinors, and increase the total population of F atoms. Furthermore, portions of the electron in the expanded and destabilized $7p_{3/2}$ spinor move to the contracted and stabilized $7p_{1/2}$ spinor.

To consider the reaction energies for the reaction, $EF_3 \rightarrow EF + F_2$ (E = I, At, and element 117), the product molecules, EF (E = I, At, and element 117), were calculated at several levels of theory with and without the spin−orbit interactions along with nonrelativistic calculations for (117)F. Although the largest possible basis set for the available computing resources were selected to perform two-component SOPP-KRCCSD(T) calculation of $(117)F_3$ in the double group $C_{2v}$ symmetry, current basis

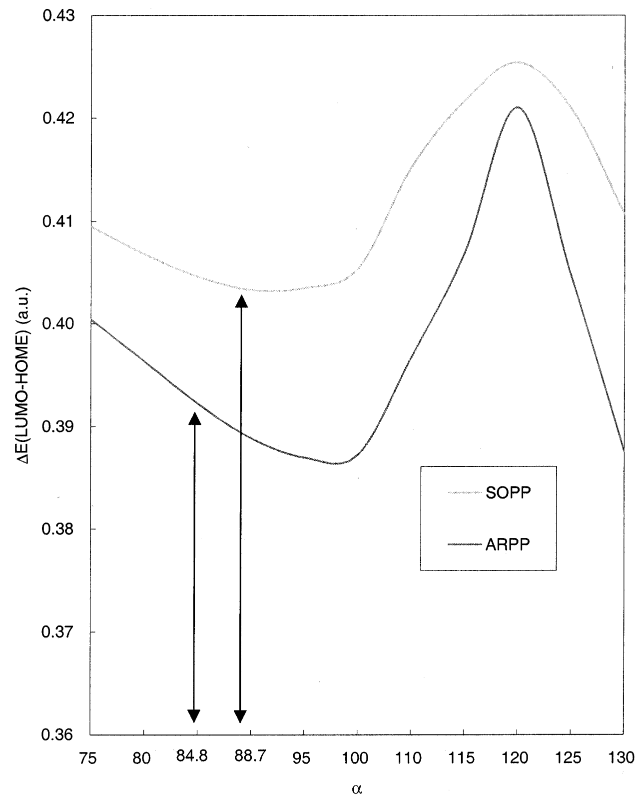


**Figure 2.** Difference between LUMO and HOMO energies (in au) of $AtF_3$ at the geometries optimized with the fixed bond angle (α).

**TABLE 5: Atomization Energies (eV) of $EF_3$ (E = I, At, and Element 117) at the Various Levels of Theory[a]**

| | method | ARPP | SOPP-KR | $\Delta_{SO}$[a] |
|---|---|---|---|---|
| $IF_3$ | HF | 1.36 | 1.12 | −0.24 |
| | MP2 | 6.56 | 6.34 | −0.22 |
| | CCSD | 5.37 | 5.14 | −0.23 |
| | CCSD(T) | 5.85 | 5.61 | −0.24 |
| $AtF_3$ | HF | 1.11 | 0.92 | −0.19 |
| | MP2 | 6.51 | 6.44 | −0.07 |
| | CCSD | 5.26 | 5.15 | −0.11 |
| | CCSD(T) | 5.76 | 5.67 | −0.09 |
| $(117)F_3$[b] | HF | 2.31 (3.04) | 3.92 (4.55) | +1.61 (+1.51) |
| | MP2 | 7.99 (8.47) | 9.24 | +1.25 |
| | CCSD | 6.67 (7.23) | 7.99 | +1.32 |
| | CCSD(T) | 7.25 (7.80) | 8.49 | +1.24 |

[a] The $\Delta_{SO}$ values are defined by the SOPP atomization energy minus the ARPP atomization energy. [b] The atomization energies in parentheses are calculated using the 4f basis on element 117.

sets are not sufficient for the accurate description of diatomic molecules, EF (E = I, At, and element 117). But the molecular trends in the group 17 fluorides $EF_3$ (E = I, At, and element 117) are, we expect, sufficiently reliable for the purpose of

**TABLE 6: Mulliken Population Analysis of $EF_3$ and EF (E = I, At, and Element 117)[a]**

| | E | | | F | |
|---|---|---|---|---|---|
| | $s$ | $p_{total}$ ($p_{1/2}$, $p_{3/2}$) | $d_{total}$ | $F^{eq}_{total}$ | $F^{ax}_{total}$ |
| $IF_3$ | 2.085 | 3.364 (1.121, 2.243) | 0.281 | 9.323 | 9.473 |
| | 2.087 | 3.355 (1.297, 2.058) | 0.280 | 9.326 | 9.476 |
| $AtF_3$ | 2.091 | 3.210 (1.070, 2.140) | 0.159 | 9.394 | 9.573 |
| | 2.099 | 3.093 (1.638, 1.455) | 0.161 | 9.442 | 9.603 |
| $(117)F_3$ | 4.118 | 9.041 (3.014, 6.027) | 10.251 | 9.528 | |
| | 4.084 | 8.781 (4.061, 4.719) | 10.262 | 9.624 | |

[a] For each molecule, the first (second) row refers to ARPP (SOPP) results.

**TABLE 7: ARPP and SOPP Reaction Energies (eV) for the Reaction $EF_3 \rightarrow EF + F_2$**

| | method | ARPP | SOPP-KR | $\Delta_{SO}$ |
|---|---|---|---|---|
| $IF_3$ | HF | 2.26 | 2.23 | −0.03 |
| | MP2 | 2.86 | 2.84 | −0.02 |
| | CCSD | 2.42 | 2.39 | −0.03 |
| | CCSD(T) | 2.45 | 2.42 | −0.03 |
| $AtF_3$ | HF | 2.13 | 2.15 | +0.02 |
| | MP2 | 2.87 | 2.99 | +0.12 |
| | CCSD | 2.39 | 2.47 | +0.08 |
| | CCSD(T) | 2.44 | 2.53 | +0.09 |
| $(117)F_3$ | HF[a] | 3.11 (3.67) | 4.41 (4.89) | +1.30 (+1.22) |
| | MP2 | 4.10 | 5.20 | +1.10 |
| | CCSD | 3.56 | 4.71 | +1.15 |
| | CCSD(T) | 3.67 | 4.75 | +1.08 |

[a] The reaction energies in parentheses are calculated using the 4f basis on Element 117.

present study. ARPP and SOPP reaction energies for the reaction $EF_3 \rightarrow EF + F_2$ (E = I, At, and element 117) are listed in Table 7. In the reaction as defined, the positive value of reaction energy means the stable $EF_3$. The reaction energies in the absence of spin−orbit interactions at the ARPP-CCSD(T) level of theory are 2.45, 2.44, and 3.67 eV for I, At, and element 117, respectively. Spin−orbit interactions slightly stabilize the product molecule for $IF_3$. In the case of $AtF_3$ and $(117)F_3$, the stabilization of the reactant molecules due to spin−orbit interactions are dominant. The stabilization is largest for element 117 and the change of the reaction energy by the spin−orbit interactions is 1.08 eV at the CCSD(T) level of theory. The SOPP-KRCCSD(T) reaction energies are 2.42, 2.53, and 4.75 eV for I, At, and element 117, respectively.

Although the $C_{2v}$ structure of $(117)F_3$ is a local minimum on the NRPP energy surface, the inclusion of relativistic effects makes the $D_{3h}$ structure of $(117)F_3$ a stable local minimum. The $(117)F_3$ molecule does not undergo Jahn−Teller distortion on the ARPP energy surface. The NRPP and ARPP energy surfaces of $(117)F_3$ in Figure 3 are for partially optimized geometries with the fixed bond angle $\alpha$. The total energy of $(117)F_3$ increases on the ARPP energy surface as the $D_{3h}$ structure distorts to the $C_{2v}$ one. The $C_{2v}$ structure of $(117)F_3$ becomes a local minimum on the NRPP energy surface at 77.7°, which is smaller than the bond angle $\alpha_e$ of $AtF_3$ (80.0°) and $IF_3$ (82.3°).[20]

The $a_1'$ occupied molecular orbital has its main contribution from the 7s orbital of element 117 and lies about 0.12 au below the $a_2''$ HOMO because of the relativistic stabilization of 7s. The 7s orbital of element 117 is stabilized by about 0.45 au due to scalar relativistic effects. If the scalar relativistic stabilization of the 7s orbital is sufficient to remove it from the valence, then the central element 117 will effectively be surrounded by five valence rather than seven valence electrons. In this situation of no s participation, VSEPR may not be operative any more. We examined NRPP and ARPP orbital

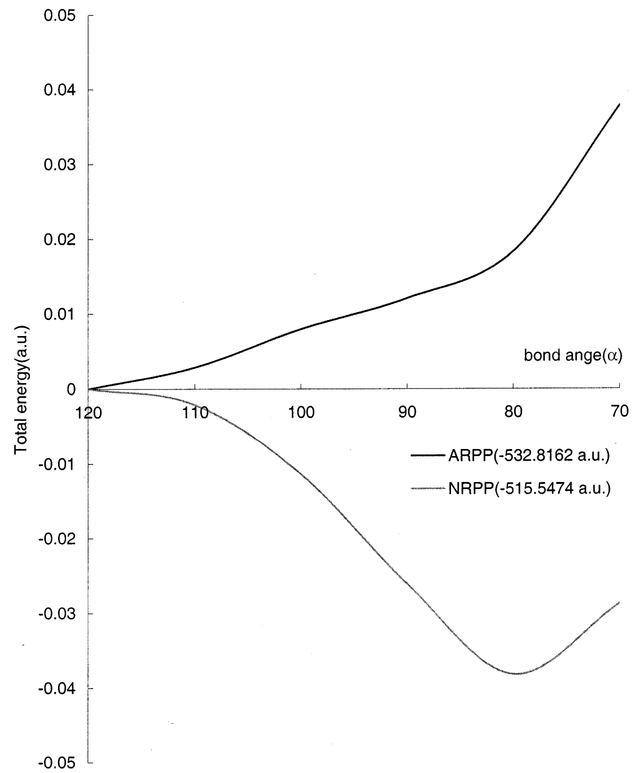


**Figure 3.** NRPP and ARPP potential energy surface of $(117)F_3$ along the bond angles ($\alpha$).

**TABLE 8: Natural Atomic Orbital Populations $(117)F_3$ in NRPP and ARPP Calculations**

| | | NRPP | | ARPP | |
|---|---|---|---|---|---|
| atom | type (AO) | occu | energy | occu | energy |
| 117 | Val (7s) | 1.77 | −0.66 | 2.00 | −1.23 |
| | Val ($7p_x$) | 1.98 | −0.40 | 0.40 | −0.17 |
| | Val ($7p_y$) | 0.31 | −0.07 | 0.40 | −0.17 |
| | Val ($7p_z$) | 0.59 | −0.16 | 2.00 | −0.47 |
| $F^{eq}$ | Val (2s) | 1.94 | −1.73 | 1.97 | −1.69 |
| | Val ($2p_x$) | 1.99 | −0.68 | 1.97 | −0.63 |
| | Val ($2p_y$) | 1.98 | −0.67 | 1.79 | −0.60 |
| | Val ($2p_z$) | 1.78 | −0.64 | 2.00 | −0.64 |
| $F^{ax}$ | Val (2s) | 1.96 | −1.70 | | |
| | Val ($2p_x$) | 1.99 | −0.64 | | |
| | Val ($2p_y$) | 1.83 | −0.62 | | |
| | Val ($2p_z$) | 1.97 | −0.64 | | |

energies of $(117)F_3$ as the $D_{3h}$ strucure distorts to $C_{2v}$. A plot of orbital energies of the valence molecular orbitals as a function of geometric parameters is called a Walsh diagram and is often employed to qualitatively explain the structure of molecules. The NRPP orbital energies of the $a_2''$ HOMO and the $a_1'$ orbital are lowered somewhat on bending, which can also be a driving force of Jahn−Teller distortion. In contrast, the ARPP orbital energies are not affected by bending.

We use the natural bond orbital (NBO) methods[39] to analyze the bond character of $(117)F_3$ in NRPP and ARPP calculations. Table 8 shows the natural atomic orbital (NAO) population of $(117)F_3$. The population of valence 7s orbital is 1.77 in the NRPP calculation and 2.00 in the ARPP calculation. Whereas the NRPP population of valence $7p_x$, which dominantly participates in the equatorial nonbonding, is 1.98, the ARPP population of valence $7p_z$, which is perpendicular to the molecular plane, is 2.00. Table 9 lists the NBO analysis of $(117)F_3$ in NRPP and ARPP calculations. The three bonding orbitals in NRPP and ARPP calculations have very similar ratios of

**TABLE 9: Natural Bond Orbital Analysis of $(117)F_3$ in NRPP and ARPP Calculations**

| natural bond orbital | | natural electron configuration | |
|---|---|---|---|
| orbital | energy | hybrids | ratio of bonding |
| | | NRPP | |
| lone pair (117) | −0.40 | p(99%), d(1%) | |
| lone pair (117) | −0.69 | s(86%), p(14%), d(1%) | |
| bonding (117−$F^{ax}$) | −0.96 | 117: s(9%), p(60%), d(18%), f(13%) | 9% |
| | | F: s(20%), p(80%) | 91% |
| bonding (117−$F^{ax}$) | −0.96 | 117: s(9%), p(60%), d(18%), f(13%) | 9% |
| | | F: s(20%), p(80%) | 91% |
| bonding (117−$F^{eq}$) | −1.01 | 117: s(9%), p(62%), d(13%), f(16%) | 12% |
| | | F: s(20%), p(80%) | 88% |
| | | ARPP | |
| lone pair (117) | −0.47 | p(100%) | |
| bonding (117−F) | −0.82 | 117: s(5%), p(66%), d(8%), f(21%) | 10% |
| | | F: s(13%), p(87%) | 90% |
| bonding (117−F) | −0.82 | 117: s(5%), p(66%), d(8%), f(21%) | 10% |
| | | F: s(13%), p(87%) | 90% |
| bonding (117−F) | −0.82 | 117: s(5%), p(66%), d(8%), f(21%) | 10% |
| | | F: s(13%), p(87%) | 90% |
| lone pair (117) | −1.23 | s(100%) | |

∼10% element 117 and ∼90% F atoms. Whereas two lone-pair orbitals of the central element 117 in the NRPP calculation are the hybrids of 7s, 7p, and 7d orbitals, two lone-pair orbitals of the $D_{3h}$ structure in the ARPP calculation are pure 7s or $7p_z$ orbitals. Two lone-pair orbitals from the central element 117 have higher energies than three bonding orbitals in the NRPP calculation, but the pure 7s lone-pair orbital has a lower energy than three bonding orbitals in the ARPP calculation. In the NRPP calculation the central element 117 has seven valence electrons, i.e., five valence electron pairs, which are three bonding pairs and two nonbonding pairs. VSEPR predicts that two hybrid lone pairs are located in equatorial positions of a trigonal bipyramid, two bonding pairs in two axial positions and one bonding in the equatorial position. The distortion from lone pair repulsion causes the axial F atoms to be bent from linear arrangement so that $EF_3$ molecules are slightly bent T $C_{2v}$ structures in the NRPP calculation. The bending is expected to increase as the central atom changes from chlorine to element 117 if one considers the size of orbital as a major factor. This trend is followed in NRPP structures. In the relativistic calculations, the 7s orbital of element 117 is stabilized enough to be removed from the valence space by scalar relativistic effects. The lone-pair orbital composed of pure 7s orbital seems to act as a core orbital. The central element 117 is effectively surrounded by five valence electrons. Two of the five valence electrons occupy the nonbonding $p_z$ orbital located perpendicular to the molecular plane and the remaining three electrons participate in three bonding orbitals located in the molecular plane. According to the VSEPR model, one may expect the $C_{3v}$ structure as a local minimum for $(117)F_3$ with four valence electron pairs, but the $D_{3h}$ structure is the only local minimum on the ARPP surface. VSEPR may not be appropriate to explain the molecular structure in this situation of no s participation.

## 4. Conclusions

We optimized geometries of $EF_3$ (E = I, At, and element 117) molecules with and without spin−orbit effects at the HF level and performed the HF normal-mode analysis. The energetics of $EF_3$ (E = I, At, and element 117) were determined from MP2, CCSD, and CCSD(T) single-point calculations with and without spin−orbit interactions. Results of two-component geometry optimization for the $EF_3$ molecules indicate that spin−orbit interactions elongate the bond lengths and widen the bond angle of $C_{2v}$ structures of $IF_3$ and $AtF_3$. Spin−orbit effects diminish the SOJT term. The bond angle $\alpha_e$ of $AtF_3$ increases by 3.9° due to spin−orbit interactions in addition to the increase of 4.8° by scalar relativistic effects, indicating that the consideration of spin−orbit effects on the geometry of $AtF_3$ is important. In the nonrelativistic scheme, all $EF_3$ (E = I, At, and element 117) molecules have $C_{2v}$ structures. The inclusion of relativistic effects make the $D_{3h}$ structure of $(117)F_3$ a stable local minimum, whereas $IF_3$ and $AtF_3$ retain $C_{2v}$ local minima even with relativistic effects. This is, to the best of our knowledge, the first molecule of the group 17 element for which the shape of most stable isomer changes by the scalar relativistic effects. The spin−orbit interactions stabilize $(117)F_3$ by a significant margin (∼1.2 eV). The electronegative F atom can effectively polarize or attract electrons from the spin−orbit destabilized $7p_{3/2}$ spinors of $(117)F_3$. As a result, the stabilization by spin−orbit interaction for $(117)F_3$ is more dominant in the bonding molecular region than in the dissociated atomic regions.

The two-component approaches seem to be very promising for studying molecular structures, vibrational frequencies, and stabilities for polyatomic molecules containing heavy and superheavy elements. The present approach can be easily applied to the molecules with many geometrical parameters, and other works in this direction are under way.

**Acknowledgment.** This work was, in part, supported by the KOSEF (1999-2-121-005-3), Center for Nanotubes and Nanostructure Composites and the Supercomputing Application Support Program of Korea Research and Development Information Center (KORDIC). We are grateful to Prof. Peter Schwerdtfeger for helpful discussions.

## References and Notes

(1) Gillespie, R. J.; Hargittai, I. *The VSEPR Model of Molecular Geometry*; Allyn and Bacon: Boston, 1991.
(2) Gillespie, R. J.; S.Nyholm, R. *Q. Rev. Chem. Soc.* **1957**, page 339.
(3) Gillespie, R. J.; Robinson, E. A. *Angew. Chem., Int. Ed. Engl.* **1996**, *35*, 495.
(4) Bersuker, I. B. *Chem. Rev.* **2001**, *101*, 1067.
(5) Bersuker, I. B. *The Jahn−Teller Effect and Vibronic Interactions in Modern Chemistry*; Plenum: New York, 1984.
(6) Bersuker, I. B.; Polinger, V. Z. *Vibronic Interaction in Molecules and Crystals*; Springer-Verlag: New York, 1989.
(7) Englman, R. *Jahn−Teller Effect*; Wiley: New York, 1972.
(8) Hirao, K.; Taketsugu, T. *The Transition State, A Theoretical Approach*; Kodansha: Tokyo, 1999.
(9) Öpik, U.; Pryce, M. H. L. *Proc. R. Soc.* **1957**, page 425.
(10) Bader, R. F. W. *Mol. Phys.* **1960**, *3*, 137.
(11) Bader, R. F. W. *Can. J. Chem.* **1962**, *40*, 1164.

(12) Pearson, R. G. *J. Am. Chem. Soc.* **1969**, *91*, 1252.
(13) Pearson, R. G. *Symmetry Rules for Chemical Reactions*; John Wiley and Sons: New York, 1976.
(14) Salem, L. *Chem. Phys. Lett.* **1969**, *3*, 99.
(15) Burdett, J. K. *Chem. Soc. Rev.* **1978**, page 507.
(16) Hoyer, S.; Seppelt, K. *Angew. Chem., Int. Ed.* **2000**, *39*, 1448.
(17) Boldyrev, A. I.; Zhdankin, V. V.; Simons, J.; Stang, P. J. *J. Am. Chem. Soc.* **1992**, *114*, 10569.
(18) Bartell, L. S.; Gavezotti, A. *THEOCHEM* **1983**, *91*, 331.
(19) Landrum, G. A.; Goldberg, N.; Hoffmann, R.; Minyaev, R. M. *New J. Chem.* **1998**, *22*, 883.
(20) Schwerdtfeger, P. *J. Phys. Chem.* **1996**, *100*, 2968.
(21) Saue, T.; Fægri, K.; Gropen, O. *Chem. Phys. Lett.* **1996**, *263*, 360.
(22) Nash, C. S.; Bursten, B. E. *J. Phys. Chem. A* **1999**, *103*, 632.
(23) Han, Y. K.; Bae, C.; Lee, Y. S. *J. Chem. Phys.* **1999**, *110*, 8969.
(24) Han, Y. K.; Bae, C.; Son, S. K.; Lee, Y. S. *J. Chem. Phys.* **2000**, *112*, 2684.
(25) K. Fægri, J.; Saue, T. *J. Chem. Phys.* **2001**, *115*, 2456.
(26) Nash, C. S.; Bursten, B. E. *Angew. Chem., Int. Ed. Engl.* **1999**, *38*, 151.
(27) Han, Y. K.; Lee, Y. S. *J. Phys. Chem. A* **1999**, *103*, 1104.
(28) Pyykkö, P.; Stoll, H. *R. S. C. Specialist Periodical Reports, Chemical Modelling, Applications and Theory*; Royal Society of Chemistry: London, 2000; Vol. 1.
(29) Lee, S. Y.; Lee, Y. S. *J. Comput. Chem.* **1992**, *13*, 595.
(30) Lee, S. Y.; Lee, Y. S. *Chem. Phys. Lett.* **1991**, *187*, 302.
(31) Kim, M. C.; Lee, S. Y.; Lee, Y. S. *Chem. Phys. Lett.* **1996**, *253*, 216.
(32) Lee, H. S.; Han, Y. K.; Kim, M. C.; Bae, C.; Lee, Y. S. *Chem. Phys. Lett.* **1998**, *293*, 97.
(33) Schwerdtfeger, P.; Seth, M. *The Encyclopedia of Computational Chemistry*; Wiley: New York, 1998; Vol.4, page 2480.
(34) Han, Y. K.; Bae, C.; Lee, Y. S.; Lee, S. Y. *J. Comput. Chem.* **1998**, *19*, 1526.
(35) Kim, Y. S.; Lee, S. Y.; Oh, W. S.; Park, B. H.; Han, Y. K.; Park, S. J.; Lee, Y. S. *Int. J. Quantum Chem.* **1998**, *66*, 91.
(36) Küchle, W.; Dolg, M.; Stoll, H.; Preuss, H. *Mol. Phys.* **1991**, *74*, 1245.
(37) Seth, M. The Chemistry of Superheavy Elements. Ph.D. Thesis, The University of Auckland, 1998.
(38) Krishnan, R.; Binkley, J. S.; Seeger, R.; Pople, J. A. *J. Chem. Phys.* **1980**, *72*, 650.
(39) Reed, A. E.; Curtiss, L. A.; Weinhold, F. *Chem. Rev.* **1988**, *88*, 899.
(40) Frisch, M. J.; Trucks, G. W.; Schlegel, H. B.; Scuseria, G. E.; Robb, M. A.; Cheeseman, J. R.; Zakrzewski, V. G.; Montgomery, J. A., Jr.; Stratmann, R. E.; Burant, J. C.; Dapprich, S.; Millam, J. M.; Daniels, A. D.; Kudin, K. N.; Strain, M. C.; Farkas, O.; Tomasi, J.; Barone, V.; Cossi, M.; Cammi, R.; Mennucci, B.; Pomelli, C.; Adamo, C.; Clifford, S.; Ochterski, J.; Petersson, G. A.; Ayala, P. Y.; Cui, Q.; Morokuma, K.; Malick, D. K.; Rabuck, A. D.; Raghavachari, K.; Foresman, J. B.; Cioslowski, J.; Ortiz, J. V.; Stefanov, B. B.; Liu, G.; Liashenko, A.; Piskorz, P.; Komaromi, I.; Gomperts, R.; Martin, R. L.; Fox, D. J.; Keith, T.; Al-Laham, M. A.; Peng, C. Y.; Nanayakkara, A.; Gonzalez, C.; Challacombe, M.; Gill, P. M. W.; Johnson, B. G.; Chen, W.; Wong, M. W.; Andres, J. L.; Head-Gordon, M.; Replogle, E. S.; Pople, J. A. *Gaussian 98*, revision A.7; Gaussian, Inc.: Pittsburgh, PA, 1998.
(41) MOLPRO is a package of ab initio programs written by H.-J. Werner and P. J. Knowles with contributions from J. Almlöf, R. D. Amos, A. Berning, D. L. Cooper, M. J. O. Deegan, A. J. Dobbyn, F. Eckert, S. T. Elbert, C. Hampel, R. Lindh, A. W. Lloyd, W. Meyer, A. Nicklass, K. Peterson, R. Pitzer, A. J. Stone, P. R. Taylor, M. E. Mura, P. Pulay, M. Schütz, H. Stoll, and T. Thorsteinsson.
(42) DiLabio, G. A.; Christiansen, P. A. *J. Chem. Phys.* **1998**, *108*, 7527.